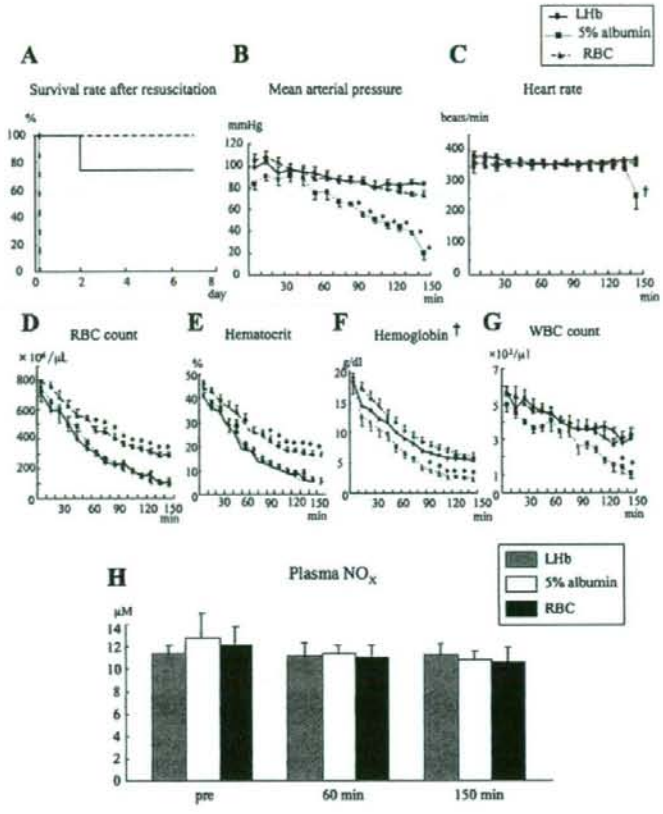

FIGURE 2. Comparisons among the rats given a transfusion of LHb, 5% albumin, or RBCs. The effect of LHb transfusion on survival after resuscitation (A), mean arterial pressure (B) and heart rates (C) as well as the changes in RBC counts (D), hematocrit levels (E), hemoglobin concentrations (F), WBC counts (G), and plasma NOx levels (H) in rats undergoing progressive hemodilution are shown. Rats underwent blood withdrawal at 0.2 mL/min via the femoral artery and simultaneous fluid resuscitation with LHb, 5% albumin, or washed rat RBCs at 0.2 mL/min via the femoral vein for 150 minutes. †Hemoglobin concentrations in the LHb-transfused rats were not actual, but estimated. Estimated Hb concentration in the LHb-transfused rats was obtained as has been described in the Methods. The data are the mean ± SE from 15 rats in each group. $*P < 0.01$, $\dagger P < 0.05$ versus other groups.

TABLE 1. Parameters of Metabolic Acidosis, Neuroendocrine Response, and Organ Dysfunction at the End of the Progressive Hemodilution Period In Rats

	LHb (n = 15)	5% Albumin (n = 15)	RBC (n = 15)	Normal Levels (n = 5)
Plasma lactate (mg/mL)	29.3 ± 2.0	130.0 ± 12.2*	29.1 ± 3.3	31.2 ± 3.2
pH	7.5 ± 0.1	7.3 ± 0.1†	7.4 ± 0.1	7.6 ± 0.2
Base excess (mmol/L)	−7.2 ± 2.2	−18.3 ± 2.5†	−7.9 ± 0.2	0.9 ± 0.4
Plasma epinephrine (ng/mL)	1.9 ± 0.5§	45.7 ± 2.2*	0.2 ± 0.1	—
Plasma norepinephrine (ng/mL)	11.9 ± 1.0§	64.0 ± 3.2*	2.0 ± 0.5	0.2 ± 0.1
Plasma C3a (μg/mL)	3.0 ± 0.5	4.2 ± 0.8‡	2.5 ± 0.2	2.0 ± 0.6
Serum H-FABP (ng/mL)	9.9 ± 0.1	38.5 ± 3.4*	8.0 ± 3.4	0.5 ± 0.2
Ejection fraction (%)	91.0 ± 2.4	42.5 ± 0.4*	94.7 ± 1.3	83.5 ± 2.5
Serum creatinine (mg/mL)	0.37 ± 0.06	0.70 ± 0.02*	0.45 ± 0.03	0.48 ± 0.07
Serum ALT (U/L)	18.0 ± 8.0	17.0 ± 2.9	15.8 ± 3.8	17.5 ± 2.6
BALF protein (mg/mL)	12.6 ± 1.6	1.2 ± 0.7†	17.5 ± 5.1	1.1 ± 1.8
Pulmonary W/D ratio	7.5 ± 0.3	6.7 ± 0.3†	7.8 ± 0.5	3.8 ± 0.8
$AaDO_2$ (torr)	39.0 ± 8.4	17.6 ± 5.4‡	46.3 ± 5.4	11.1 ± 1.6

Rats underwent blood withdrawal at 0.2 mL/min via the femoral artery and simultaneous fluid resuscitation with LHb, 5% albumin, or washed RBCs at 0.2 mL/min via the femoral vein for 150 min. At the end of the 150-min period, samples of blood and BALF were obtained and used to measure the parameters. Ejection fraction, PaO_2 and $PaCO_2$ were also measured at the end of hemodilution. $AaDO_2$ was calculated using the equation presented in the Methods. Normal levels were obtained from non-treated normal rats. Data are mean ± SE.

$*P < 0.01$, $\dagger P < 0.05$ versus other groups, $\S P < 0.01$, $\ddagger P < 0.05$ versus RBC.

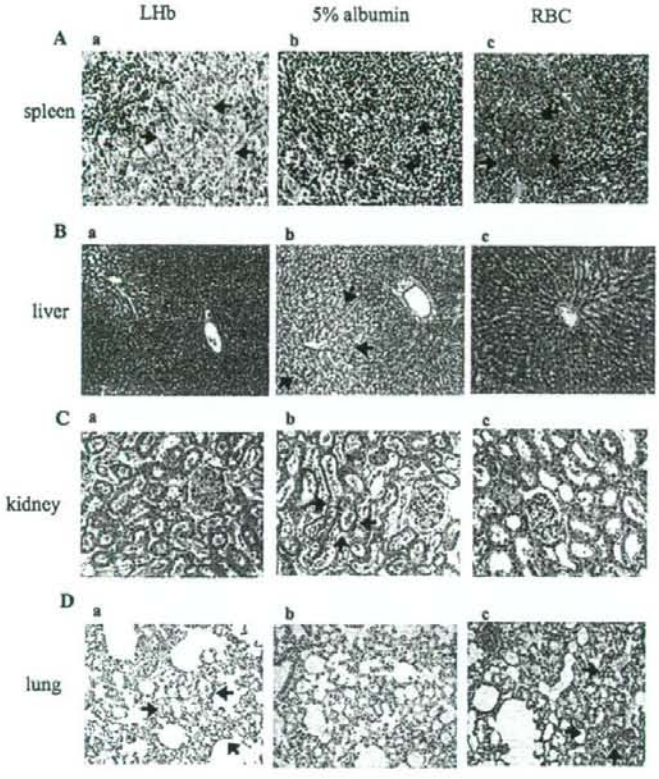

FIGURE 3. Pathologic findings at the end of the transfusion with LHb, 5% albumin, or washed rat RBCs. Blood withdrawal and fluid resuscitation were performed for 150 minutes as has been described in Figures 2A, B, and C. At 150 minutes after the start of the progressive hemodilution, the following organs were removed from the rats: spleen, liver, kidney, lung. panels A and C, ×400, H.E.; panels B and D, ×200, H.E.

fused rats also showed significantly lower serum creatinine concentrations than the albumin-transfused rats, with levels similar to the normal level (Table 1), demonstrating prevention of renal dysfunction. There were no increases for the serum ALT concentrations in any of the transfused rat groups after 150 minutes (Table 1), with normal ALT levels seen in all of the groups (Table 1). As compared with the albumin-transfused rats, both LHb- and RBC-transfused rats unexpectedly had significantly higher protein concentrations in the BALF, along with higher pulmonary wet/dry ratios and $AaDO_2$ values. Since these parameters were also higher than the normal levels, this proves that there was an increased pulmonary dysfunction (Table 1).

Histopathology of the Spleen, Liver, Kidneys, and Lungs at the End of Transfusion

The red pulp zones of the spleens of the LHb-transfused rats were filled with a large amount of LHb, but not RBCs (Fig. 3A-a, indicated by the arrows) at the end of the transfusion. The red pulp zone of the RBC-transfused rats was also filled with a substantial amount of RBCs (Fig. 3A-c, indicated by arrows). The albumin-transfused rats only had a few RBCs in the red pulp zone (Fig. 3A-b, indicated by arrows). The livers of the albumin-transfused rats showed an apparent sinusoidal dilation and marked vacuolar degeneration of the hepatocytes, particularly around the central veins (Fig. 3B-b, indicated by arrows). However, the livers of both the LHb- and RBC-transfused rats did not manifest such severe ischemic changes (Figs. 3B-a, c). The albumin-transfused rats also showed acute tubular necrosis in the kidney (Fig. 3C-b, indicated by arrows), which was in contrast to the LHb-and RBC-transfused rats (Figs. 3C-a, c). The LHb- and RBC-transfused rats (Figs. 3D-a, c; indicated by the arrows), but not the albumin-transfused rats (Fig. 3D-b), showed mild to moderate pulmonary edema in the lung.

LHb Transfusion Attenuates HIF-1alpha Expression in the Liver and Kidney of Rats Undergoing Progressive Hemodilution

The albumin-transfused rats showed strong HIF-1alpha staining in the hepatocyte nuclei, particularly around the central veins at the end of the exchange transfusion period (Fig. 4A-b, indicated by arrows), whereas the LHb-transfused rats only showed a weak HIF-1alpha staining in the nuclei around the central veins (Fig. 4A-a, indicated by arrows). There was no staining noted for the liver of the RBC-transfused rats (Fig. 4A-c). The proximal convoluted tubules of the kidneys in the albumin-transfused rats also showed strong HIF-1alpha staining (Fig. 4B-b, indicated by arrows),

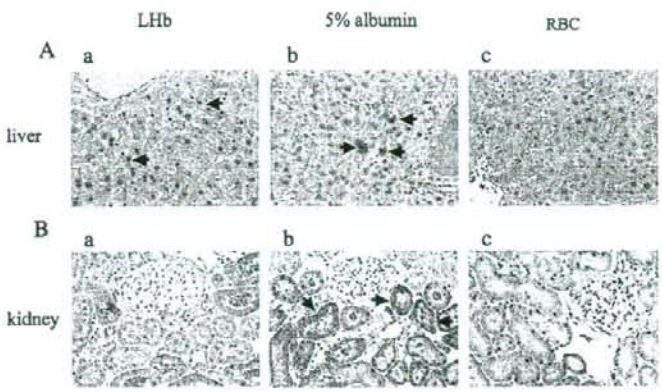

FIGURE 4. Immunohistochemistry for HIF-1alpha protein in the liver (A) and kidney (B) after transfusion with LHb, 5% albumin, or washed rat RBCs. Blood withdrawal and fluid resuscitation were performed for 150 minutes as has been described in Figures 2A-G. After progressive hemodilution, the livers and kidneys were removed from the rats to stain for HIF-1alpha protein by immunohistochemistry. Magnification, ×1,000.

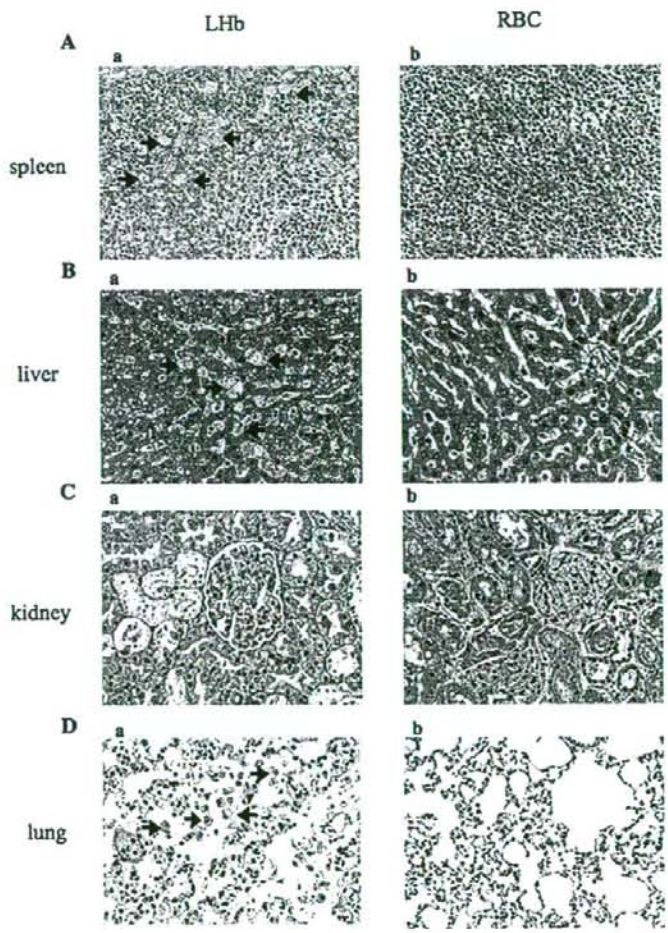

FIGURE 5. Pathologic findings of the LHb-transfused rats and the washed RBC-transfused rats at 48 hours after the progressive hemodilution. The spleens, livers, kidneys, and lungs were removed from the rats at 48 hours after the hemodilution. Magnification, ×400; H.E.

whereas the LHb- and the RBC-transfused rats exhibited little staining in comparison (Figs. 4B-a, c). Neither the spleens nor the lungs showed positive staining for HIF-1alpha in any of the transfused rat groups (data not shown).

Mortality and Marked Activation of Phagocytic Macrophages in the Spleens, Livers, and Lungs of LHb-Transfused Rats at 48 Hours After Transfusion

In 4 of the 15 LHb-transfused rats, the animals died within 48 hours after hemodilution. As to the cause of death, they manifested significant splenomegaly compared with the RBC-transfused rats at 48 hours after the progressive hemodilution. Histopathology revealed a remarkable increase of phagocytic macrophages in the spleen of these animals, which also had phagocytized LHb vesicles (Fig. 5A-a, indicated by arrows). In contrast, no erythrophagocytosis was seen in the spleens of the RBC-transfused rats (Fig. 5A-b). A substantial number of Kupffer cells were observed in the livers of the LHb-transfused rats, which also had phagocytized LHb vesicles (Fig. 5B-a, indicated by arrows), whereas the livers of the RBC-transfused rats only showed sinusoidal dilation (Fig. 5B-b). There were no significant lesions observed in the kidneys of either the LHb- or RBC-transfused rats (Figs. 5C-a, b). The lungs of the LHb-transfused rats (Fig. 5D-a, indicated by arrows) but not the RBC-transfused rats (Fig. 5D-b) had increased numbers of alveolar macrophages with mild alveolar septal thickness.

DISCUSSION

LHb transfusion can effectively rescue rats from fatal progressive hemodilution without the presence of any potent NO scavenging effect, and thus, can dramatically improve the anaerobic abnormalities induced by progressive hemodilution in rats. This indicates that LHb can satisfactorily play a role as an oxygen carrier. The findings of the present study that examined LHb transfusions, especially the results for the HIF-1alpha expression, strongly support the salutary effects of LHb transfusions on the microcirculation. The heterodimer HIF-1, which is composed of alpha and beta subunits, is the main molecular transducer of hypoxic signals.[26] During hypoxia, cytoplasmic HIF-1alpha is imported into the nuclei, which leads to the generation of a DNA binding complex along with HIF-1beta.[27] Thus, after moving into the nuclei HIF-1alpha is activated. These mechanisms have been recognized as the major mediators of the acute response to hypoxia in organs and cultured cells.[28]

In rats undergoing progressive hemodilution, it is possible that the LHb transfusion does not affect the plasma NO metabolite (NOx) concentrations, which includes the NO metabolites and also reflects the local NO concentration. If so, this indicates that LHb attenuates the harmful effect of acellular Hb on vasoconstriction, as it does not have a potent NO scavenging effect. The NOx levels in the plasma have been used as an index of NO concentration in the endothelial cells, especially within the local circulation.[29] Due to the NO scavenging effect noted to be associated with various acellular Hb solutions, administration of these solutions might possibly induce vasoconstriction.[7,8] The consequence of such a vasoconstriction would be the collapse of the arteriolar circulation that provides oxygen to the tissues. If precapillary arterioles are constricted by the lack of NO that is scavenged, they lose their pressurization and collapse. The surface modification that occurs with polyethylene glycol is additionally beneficial in that it not only causes a longer circulation time,[30] but it also helps in suppressing vesicular aggregation of LHb in the circulation.[31] This may help to explain why LHb transfusion did not affect the plasma NOx levels.

Among the current RBC substitutes, Hb-based oxygen carriers have been classified based on their structural characteristics and include polymerized bovine or human Hb, PEG-modified Hb, or LHb, which was used in the present study. Although the polymerized bovine Hb, Hemopure (Biopure Co., Cambridge, MA), has undergone extensive clinical studies for safety,[32–34] several studies have raised the concern about increased systemic vascular resistance,[35,36] which is possibly related to the NO scavenging by the free Hb. However, it is noteworthy that Hemopure has been approved for replacement of acute blood loss in South Africa.[37] Polymerized human Hb, PolyHeme (Northfield Laboratory, Evanston, IL), has also undergone many clinical studies,[5,6,38–40] including recent phase III trials.[5,6] Although Moore et al have demonstrated that significant vasoconstrictor effects were not observed in patients after the administration of PolyHeme,[5,6,38] some investigators have examined its vasopressor effect.[4] Hemolink (Hemosol Inc., Toronto, Canada) is a oligomerized human Hb cross-linked with the oxidized trisaccharide *o*-raffinose.[41] In a recent phase II clinical trial of Hemolink, an increased blood pressure was reported.[42] Hemospan (Sangart Inc., San Diego, CA) is a human Hb modified by the surface conjugation of monofunctional maleimide-activated 5-kDa PEG to surface thiol groups.[9,10] Vandegriff et al have demonstrated that Hemospan does not exhibit the typical hypertensive response that is observed with most acellular Hb solutions.[9,10] However, as many animal studies on Hemospan did not examine the NO/NOx levels, the effect of Hemospan on NO scavenging has yet to be discerned.[9,10,43] A recent phase II clinical trial of Hemospan suspected that there was the possibility of a Hemospan-related hypertension.[44] In contrast, even though clinical trials for LHb have yet to be started, we, along with other investigators, have demonstrated that LHb does not have either a significant vasoconstrictor effect[12–16,45] or a NO scavenging effect. Thus, for LHb, it is important that clinical studies be undertaken in humans to confirm the current findings for this new Hb-based oxygen carrier. If further clinical trials are performed in a larger number of patients, this should answer the questions that still remain concerning this compound.

The reason why the Hb concentration of LHb is almost half of the conventional packed human RBC unit can be explained by the excellent oxygen carrying capacity that is found for LHb. The P_{50} of the LHb used in this study was adjusted to 40 to 50 mm Hg, in contrast to the 27 to 28 mm Hg that is found in normal human RBCs. Basically, LHb is intended for use in patients with massive hemorrhage. Such critical patients usually receive high concentration oxygen

therapy. When a patient without respiratory disease is given 40% oxygen, his or her PaO_2 could conceivably reach nearly 200 mm Hg, with a PvO_2 of almost 40 mm Hg. Under such conditions, the oxygen transporting efficiency (OTE) of LHb is approximately 50%, while that for the normal human RBCs is about 25%. In other words, LHb has a 2-fold higher OTE than normal RBCs. Because of this, we prepared an LHb product that had an Hb concentration of 6 g/dL, which is 50% of a conventional packed allogenic RBC unit (Hb concentration 12 g/dL). In the current study, the P_{50} of normal rat RBCs was approximately 38%, with the OTEs of the LHb and rat RBCs approximately 50% with mechanical ventilation when using room air (PaO_2, 110–120 mm Hg; PvO_2, 30 mm Hg). Therefore, we adjusted the Hb concentration of the washed rat RBCs to 6 g/dl, to create conditions that were similar to the LHb.

Despite its ameliorating effects for tissue hypoxia, the LHb transfusion did not prevent acute lung injury. Although the mechanism for this was not clear, the RBC-transfused rats also exhibited a similar acute lung injury. In a recent review, it has been demonstrated that massive transfusion might be a definite risk factor for acute lung injury.[46] Massive transfusion of artificial or allogenic blood products might directly lead to acute lung injury. The LHb-transfused rats, as well as the RBC-transfused rats, also had higher WBC counts at the end of the exchange transfusion period when compared with that seen for the albumin-transfused rats, which is in agreement with a previous report.[46] We presume that a massive transfusion with LHb or RBC induces certain inflammatory mediators that are involved in increasing the WBC count, which leads to the occurrence of acute lung injury. Further investigations are needed to be able to verify the mechanisms responsible for the increased WBCs and acute lung injuries that are associated with massive LHb transfusions.

When LHb is administered in a clinical setting, there are several concerns that need to be taken into consideration. First, the half-life of LHb is relatively short. Despite the initial success of the LHb resuscitation, 4 of 15 LHb-transfused rats died within 48 hours after the hemorrhage/transfusion. Because the biologic half-life of LHb is estimated to be approximately 13 hours, we presumed that one of the causes of death in the LHb-transfused rats was due to the severe anemia that resulted from the destruction of LHb. Second, large amounts of liposome capsule remain in the host after massive LHb transfusions. It has been speculated that some of the liposomes are capable of activating the complement system.[25] However, we did not observe any elevated plasma C3a concentrations after our LHb infusion. Third, LHb strongly activates/stimulates the reticuloendothelial system after the initial resuscitation. Sakai et al has reported that Hb encapsulated vesicles are exclusively degraded by the reticuloendothelial systems.[14,47] Based on our findings of an exaggerated increase of the number of Kupffer cells, we speculate that the liver has no additional capacity to phagocytize/detoxify foreign bodies or harmful substances, and thus, we propose the maintenance of a host's defense system that is the most important factor after an initial successful resuscitation using this LHb transfusion.

REFERENCES

1. Przybelski RJ, Malcolm DS, Burris DG, et al. Cross-linked hemoglobin solution as a resuscitative fluid after hemorrhage in the rat. *J Lab Clin Med.* 1991;117:143–151.
2. Schultz SC, Powell CC, Burris DG, et al. The efficacy of diaspirin crosslinked hemoglobin solution resuscitation in a model of uncontrolled hemorrhage. *J Trauma.* 1994;37:408–412.
3. Sloan EP, Koenigsberg M, Gens D, et al. Diaspirin cross-linked hemoglobin (DCLHb) in the treatment of severe traumatic hemorrhagic shock: a randomized controlled efficacy trial. *Jama.* 1999;282:1857–1864.
4. Handrigan MT, Bentley TB, Oliver JD, et al. Choice of fluid influences outcome in prolonged hypotensive resuscitation after hemorrhage in awake rats. *Shock.* 2005;23:337–343.
5. Gould SA, Moore EE, Hoyt DB, et al. The first randomized trial of human polymerized hemoglobin as a blood substitute in acute trauma and emergent surgery. *J Am Coll Surg.* 1998;187:113–120, discussion 120–122.
6. Moore EE, Cheng AM, Moore HB, et al. Hemoglobin-based oxygen carriers in trauma care: scientific rationale for the us multicenter prehospital trial. *World J Surg.* 2006;30:1247–1257.
7. Schultz SC, Grady B, Cole F, et al. A role for endothelin and nitric oxide in the pressor response to diaspirin cross-linked hemoglobin. *J Lab Clin Med.* 1993;122:301–308.
8. Doherty DH, Doyle MP, Curry SR, et al. Rate of reaction with nitric oxide determines the hypertensive effect of cell-free hemoglobin. *Nat Biotechnol.* 1998;16:672–676.
9. Tsai AG, Vandegriff KD, Intaglietta M, Winslow RM. Targeted O2 delivery by low-P50 hemoglobin: a new basis for O2 therapeutics. *Am J Physiol Heart Circ Physiol.* 2003;285:H1411–H1419.
10. Vandegriff KD, Malavalli A, Wooldridge J, et al. MP4, a new nonvasoactive PEG-Hb conjugate. *Transfusion.* 2003;43:509–516.
11. Bjorkholm M, Fagrell B, Przybelski R, et al. A phase I single blind clinical trial of a new oxygen transport agent (MP4), human hemoglobin modified with maleimide-activated polyethylene glycol. *Haematologica.* 2005;90:505–515.
12. Ogata Y, Goto H, Kimura T, Fukui H. Development of neo red cells (NRC) with the enzymatic reduction system of methemoglobin. *Artif Cells Blood Substit Immobil Biotechnol.* 1997;25:417–427.
13. Sakai H, Takeoka S, Park SI, et al. Surface modification of hemoglobin vesicles with poly(ethylene glycol) and effects on aggregation, viscosity, and blood flow during 90% exchange transfusion in anesthetized rats. *Bioconjug Chem.* 1997;8:23–30.
14. Sakai H, Horinouchi H, Tomiyama K, et al. Hemoglobin-vesicles as oxygen carriers: influence on phagocytic activity and histopathological changes in reticuloendothelial system. *Am J Pathol.* 2001;159:1079–1088.
15. Oda T, Nakajima Y, Kimura T, et al. Hemodilution with liposome-encapsulated low-oxygen-affinity hemoglobin facilitates rapid recovery from ischemic acidosis after cerebral ischemia in rats. *J Artif Organs.* 2004;7:101–106.
16. Oda T, Kimura T, Ogata Y, Fujise Y. Hemodilution with liposome-encapsulated low-oxygen-affinity hemoglobin does not attenuate hypothermic cerebral ischemia in rats. *J Artif Organs.* 2005;8:263–269.
17. Sakai H, Masada Y, Horinouchi H, et al. Hemoglobin-vesicles suspended in recombinant human serum albumin for resuscitation from hemorrhagic shock in anesthetized rats. *Crit Care Med.* 2004;32:539–545.
18. Sakai H, Tomiyama K, Masada Y, et al. Pretreatment of serum containing hemoglobin vesicles (oxygen carriers) to prevent their interference in laboratory tests. *Clin Chem Lab Med.* 2003;41:222–231.
19. Ishibashi T, Kubota K, Himeno M, et al. Respiratory alkalosis does not alter NOx concentrations in human plasma and erythrocytes. *Am J Physiol Heart Circ Physiol.* 2001;281:H2757–H2761.
20. Ishibashi T, Yoshida J, Nishio M. New methods to evaluate endothelial function: A search for a marker of nitric oxide (NO) in vivo: re-evaluation of NOx in plasma and red blood cells and a trial to detect nitrosothiols. *J Pharmacol Sci.* 2003;93:409–416.
21. Ishibashi T, Matsubara T, Ida T, et al. Negative NO3- difference in human coronary circulation with severe atherosclerotic stenosis. *Life Sci.* 2000;66:173–184.
22. Boluyt MO, Converso K, Hwang HS, et al. Echocardiographic assess-

ment of age-associated changes in systolic and diastolic function of the female F344 rat heart. *J Appl Physiol*. 2004;96:822–828.
23. Kinoshita M, Ono S, Mochizuki H. Neutrophils mediate acute lung injury in rabbits: role of neutrophil elastase. *Eur Surg Res*. 2000;32: 337–346.
24. Kinoshita M, Seki S, Ono S, et al. Paradoxical effect of IL-18 therapy on the severe and mild Escherichia coli infections in burn-injured mice. *Ann Surg*. 2004;240:313–320.
25. Szebeni J, Fontana JL, Wassef NM, et al. Hemodynamic changes induced by liposomes and liposome-encapsulated hemoglobin in pigs: a model for pseudoallergic cardiopulmonary reactions to liposomes. Role of complement and inhibition by soluble CR1 and anti-C5a antibody. *Circulation*. 1999;99:2302–2309.
26. Wang GL, Jiang BH, Rue EA, Semenza GL. Hypoxia-inducible factor 1 is a basic-helix-loop-helix-PAS heterodimer regulated by cellular O2 tension. *Proc Natl Acad Sci USA*. 1995;92:5510–5514.
27. Semenza GL. Expression of hypoxia-inducible factor 1: mechanisms and consequences. *Biochem Pharmacol*. 2000;59:47–53.
28. Semenza GL. Regulation of mammalian O2 homeostasis by hypoxia-inducible factor 1. *Annu Rev Cell Dev Biol*. 1999;15:551–578.
29. Ellis G, Adatia I, Yazdanpanah M, Makela SK. Nitrite and nitrate analyses: a clinical biochemistry perspective. *Clin Biochem*. 1998;31: 195–220.
30. Phillips WT, Klipper RW, Awasthi VD, et al. Polyethylene glycol-modified liposome-encapsulated hemoglobin: a long circulating red cell substitute. *J Pharmacol Exp Ther*. 1999;288:665–670.
31. Sakai H, Tomiyama KI, Sou K, et al. Poly(ethylene glycol)-conjugation and deoxygenation enable long-term preservation of hemoglobin-vesicles as oxygen carriers in a liquid state. *Bioconjug Chem*. 2000;11:425–432.
32. Standl T, Burmeister MA, Horn EP, et al. Bovine haemoglobin-based oxygen carrier for patients undergoing haemodilution before liver resection. *Br J Anaesth*. 1998;80:189–194.
33. LaMuraglia GM, O'Hara PJ, Baker WH, et al. The reduction of the allogenic transfusion requirement in aortic surgery with a hemoglobin-based solution. *J Vasc Surg*. 2000;31:299–308.
34. Levy JH, Goodnough LT, Greilich PE, et al. Polymerized bovine hemoglobin solution as a replacement for allogeneic red blood cell transfusion after cardiac surgery: results of a randomized, double-blind trial. *J Thorac Cardiovasc Surg*. 2002;124:35–42.
35. Hughes GS Jr, Antal EJ, Locker PK, et al. Physiology and pharmacokinetics of a novel hemoglobin-based oxygen carrier in humans. *Crit Care Med*. 1996;24:756–764.
36. Kasper SM, Walter M, Grune F, et al. Effects of a hemoglobin-based oxygen carrier (HBOC-201) on hemodynamics and oxygen transport in patients undergoing preoperative hemodilution for elective abdominal aortic surgery. *Anesth Analg*. 1996;83:921–927.
37. Levien LJ. South Africa: clinical experience with Hemopure. *ISBT Science Series (2006)*. 2006;1:167–173.
38. Johnson JL, Moore EE, Offner PJ, et al. Resuscitation of the injured patient with polymerized stroma-free hemoglobin does not produce systemic or pulmonary hypertension. *Am J Surg*. 1998;176:612–617.
39. Johnson JL, Moore EE, Offner PJ, et al. Resuscitation with a blood substitute abrogates pathologic postinjury neutrophil cytotoxic function. *J Trauma*. 2001;50:449–455, discussion 456.
40. Gould SA, Moore EE, Hoyt DB, et al. The life-sustaining capacity of human polymerized hemoglobin when red cells might be unavailable. *J Am Coll Surg*. 2002;195:445–452, discussion 452–455.
41. Torres Filho IP, Spiess BD, Barbee RW, et al. Systemic responses to hemodilution after transfusion with stored blood and with a hemoglobin-based oxygen carrier. *Anesth Analg*. 2005;100:912–920.
42. Cheng DC, Mazer CD, Martineau R, et al. A phase II dose-response study of hemoglobin raffimer (Hemolink) in elective coronary artery bypass surgery. *J Thorac Cardiovasc Surg*. 2004;127:79–86.
43. Young MA, Riddez L, Kjellstrom BT, et al. MalPEG-hemoglobin (MP4) improves hemodynamics, acid-base status, and survival after uncontrolled hemorrhage in anesthetized swine. *Crit Care Med*. 2005;33: 1794–1804.
44. Olofsson C, Ahl T, Johansson T, et al. A multicenter clinical study of the safety and activity of maleimide-polyethylene glycol-modified Hemoglobin (Hemospan) in patients undergoing major orthopedic surgery. *Anesthesiology*. 2006;105:1153–1163.
45. Sakai H, Takeoka S, Wettstein R, et al. Systemic and microvascular responses to hemorrhagic shock and resuscitation with Hb vesicles. *Am J Physiol Heart Circ Physiol*. 2002;283:H1191–H1199.
46. Nathens AB. Massive transfusion as a risk factor for acute lung injury: association or causation? *Crit Care Med*. 2006;34(5 Suppl):S144–S150.
47. Sakai H, Horinouchi H, Yamamoto M, et al. Acute 40 percent exchange-transfusion with hemoglobin-vesicles (HbV) suspended in recombinant human serum albumin solution: degradation of HbV and erythropoiesis in a rat spleen for 2 weeks. *Transfusion*. 2006;46:339–347.

Selection of hematopoietic stem cells with a combination of galactose-bound vinyl polymer and soybean agglutinin, a galactose-specific lectin

Hirofumi Yura, Yasuhiro Kanatani, Masayuki Ishihara, Bonpei Takase, Masaki Nambu, Satoko Kishimoto, Michihiro Kitagawa, Osamu Tatsuzawa, Yasutaka Hoshi, Shinya Suzuki, Mitsuyuki Kawakami, and Takemi Matsui

BACKGROUND: Selection of hematopoietic stem cells can be used to prevent graft-versus-host disease (GVHD) after allograft transplantation. The purpose of the study was to examine a novel cell separation system comprising a galactose-bound vinyl polymer (Gal-VP) and soybean agglutinin (SBA), a galactose-specific lectin.

STUDY DESIGN AND METHODS: A vinyl polymer (VP) containing α-1,6- and β-1,4-linked galactose terminals was used to facilitate cell separation. A VP containing an α-1,4-linked glucose terminal (α-1,4-Glu-VP) was also synthesized as a control for α-1,6- and β-1,4-Gal-VP. Peripheral blood samples were collected from healthy volunteers and umbilical cord blood cells were collected after normal labor.

RESULTS: The sugar-VP was adsorbed on the surface of various materials. In the presence of SBA, T lymphocytes bound to β-1,4-Gal-VP–coated microbeads, but not to α-1,4-Glu-VP–coated microbeads. When peripheral or cord blood cells were cultured on α-1,6-Gal-VP–coated plates, most red blood cells, lymphocytes, granulocytes, and monocytes adhered to the plate in the presence of 300 mg per mL SBA, whereas few CD34+ cells attached, even with 800 mg per mL SBA.

CONCLUSION: SBA binds selectively to blood cells by recognizing cell-surface sugars, which are dependent on the extent of cellular differentiation. Therefore, the combination of α-1,6-Gal-VP and SBA might be useful for separation of blood cells according to their stage of differentiation and lineage.

Lectins are a group of proteins that bind selectively to sugar chains.[1] Lectins bind to sugar residues expressed on cell surfaces to stimulate aggregation of red blood cells (RBCs), lymphocyte proliferation, and specific aggregation of leukemic cells,[2-4] and this property of lectins has been used to separate specific cells types from heterogeneous blood cell populations.[5] The lectin most commonly used for stem cell selection is soybean agglutinin (SBA), a tetrameric glycoprotein containing four galactose-binding sites that binds specifically to D-galactose and *N*-acetyl-D-galactosamine.[6,7] The binding affinity of SBA depends on the level of galactose expression and is higher for mature cells such as RBCs, granulocytes, T lymphocytes, and

ABBREVIATIONS: Gal-VP = galactose-bound vinyl polymer; α-1,4-Glu-VP = vinyl polymer containing an α-1,4-linked glucose terminal; NK cells = natural killer cells; SBA = soybean agglutinin; VP = vinyl polymer.

From NeTech, Inc., Kawasaki, Kanagawa; Research Institute, National Defense Medical College, Tokorozawa, Saitama; the Department of Plastic and Reconstructive Surgery, National Defense Medical College, Tokorozawa, Saitama; the Graduate School of Veterinary Medicine and Life Science, Nippon Veterinary and Life Science University, Musashino-shi, Tokyo; the National Center for Child Health and Development, Setagaya-Ku, Tokyo; the Division of Blood Transfusion, Jikei University Hospital, Minato-ku, Tokyo; and the Faculty of System Design, Tokyo Metropolitan University, Hino, Tokyo, Japan.

Address reprint requests to: Yasuhiro Kanatani, MD, PhD, Research Institute, National Defense Medical College, 3-2 Namiki, Tokorozawa, Saitama 359-8513, Japan; e-mail: ykanatan@ndmc.ac.jp.

Received for publication May 8, 2007; revision received August 13, 2007, and accepted August 21, 2007.

doi: 10.1111/j.1537-2995.2007.01571.x

TRANSFUSION 2008;48:561-566.

platelets. In contrast, SBA has low affinity for immature stem cells[8] and this selectivity can be utilized to accomplish stem cell enrichment.

T-lymphocyte depletion from marrow fluid can be achieved by mixing cells with sheep RBCs and SBA to form specific aggregates. This approach has facilitated successful marrow transplantation by expanding hematopoietic stem cells and reducing graft-versus-host disease (GVHD).[9] Other trials have utilized a purging method with polystyrene culture devices carrying covalently immobilized SBA.[10]

We have developed a novel cell separation system for clinical use, with a combination of a galactose-bound vinyl polymer (Gal-PV) and SBA. This system includes a separating surface comprising a solid support, such as a column, microbeads, or a culture plate, coated with Gal-PV to bind blood cells via SBA (Fig. 1). This system has several advantages: 1) it does not require use of unstable mammalian RBCs such as sheep blood cells; 2) there is no requirement for covalent immobilization of SBA, which may reduce function; and 3) it is a simple method that does not require expensive antibodies. In this study, we examined the selectivity of sugar-PV–coated polystyrene plates for collection of blood cells in the presence of SBA. Mature peripheral blood cells (RBCs, lymphocytes, and granulocytes-monocytes) adhered preferentially to plates coated with α-1,6-Gal-PV in the presence of SBA, whereas primitive hematopoietic stem cells did not do so. Therefore, this system might be useful for separation of blood cells according to the stage of differentiation and the cell lineage.

MATERIALS AND METHODS

We used a vinyl polymer (VP) containing α-1,6- and β-1,4-linked galactose terminals to facilitate cell separation. VP containing an α-1,4-linked glucose terminal was also synthesized as a control for α-1,6- and β-1,4-galactose–bound vinyl polymer (Gal-VP). Sugar-VPs (α-1,6-Gal-VP, β-1,4-Gal-VP, and α-1,4-Glu-VP) were prepared via homopolymerization of *N*-*p*-vinylbenzyl-4-*O*-α-D-galactopyranosyl-(1,6)-D-gluconamide (Seikagaku Corp., Tokyo, Japan), and *N*-*p*-vinylbenzyl-4-*O*-β-D-galactopyranosyl-(1,4)-D-gluconamide (Seikagaku).[11] The sugar-VPs were obtained from NeTech, Inc., and their structures are shown in Fig. 2.

For immobilization, an aqueous solution of sugar-VP (10-500 mg/mL) was prepared by dissolving the required amount of each sugar-VP in distilled water. Aliquots of the solution were placed on a cell culture plate (Sumitomo

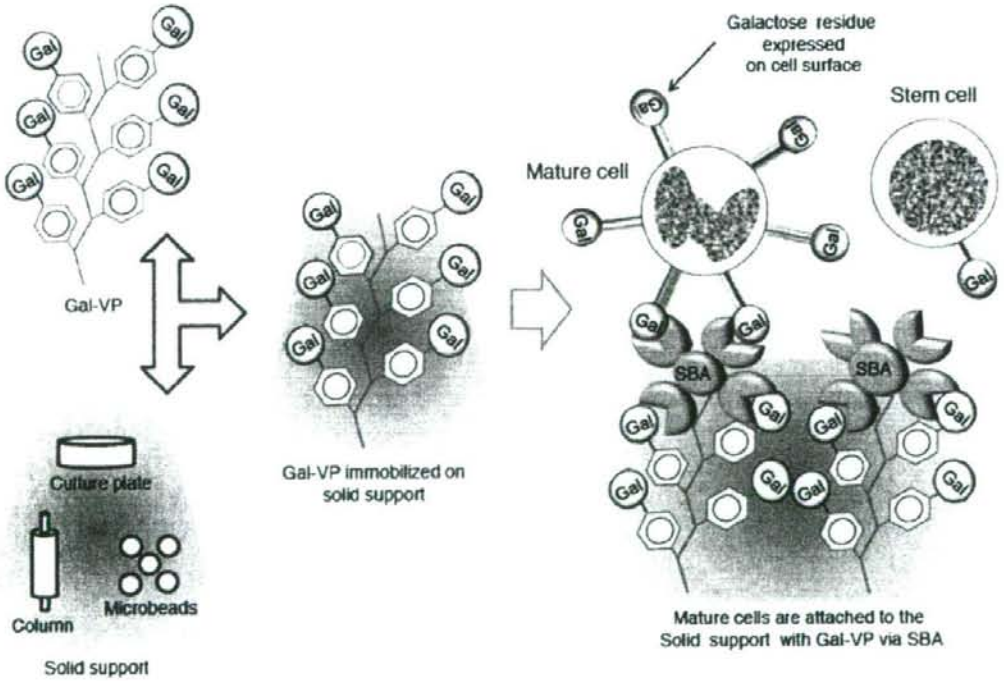

Fig. 1. Schematic illustration of the cell separation system with Gal-VP and SBA.

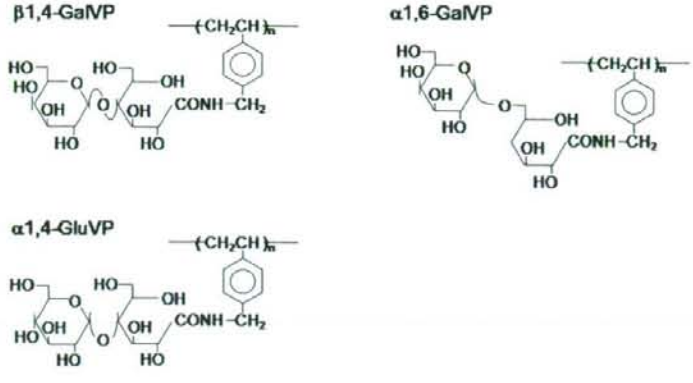

Fig. 2. Structures of sugar-VPs.

Bakelite Corp., Tokyo, Japan) or mixed with microbeads (Invitrogen, Carlsbad, CA) at room temperature for at least 2 hours. The solution was then decanted and the plates or microbeads were rinsed with PBS containing divalent cations (Ca^{2+} and Mg^{2+} Nissui Corp., Tokyo, Japan).

Fluorescein isothiocyanate (FITC; 1.28×10^{-4} mol; Wako Pure Chemical Industries, Tokyo, Japan) and dibutyltin dilaurate (Wako) were added to the sugar-VP solution (500 mg; 10^{-3} mol monomer unit) in 5 mL of dehydrated dimethyl sulfoxide containing three drops of dehydrated pyridine. The mixture was heated for 2 hours at 90°C and then poured into an excess volume of ethanol. The product was purified several times by dissolving in water and precipitating with ethanol, and the FITC-conjugated sugar-VP was finally collected by filtration. One molecule of FITC was bound to every 40 structural units of the polymer chain, as determined by fluorescence spectrometry (RF-500 spectrophotometer, Shimadzu Corp., Kyoto, Japan).

The amount of sugar-VP on the plates was estimated as follows. Aqueous solutions of FITC-conjugated sugar-VP were placed onto plates for the prescribed time periods. The solution was then removed and the plates were rinsed with distilled water. The plates were then sonicated with 500 mg per mL Tween 20 for 30 seconds. It was confirmed that the adsorbed FITC-conjugated sugar-VP had been completely removed from the plates after treatment with Tween 20 and sonication. The amount of FITC-conjugated sugar-VP was calculated from a linear correlation with fluorescence. The symbols "+++," "++," or "+" represent adsorption of sugar-VP or sugar (lactose and galactose) to various materials at levels of 0.6, 0.6 to 0.4, and 0.4 μg per cm^2, respectively.

Peripheral blood samples (7 mL) were collected from healthy volunteers into Vacutainer tubes containing ethylenediaminetetraacetate (Terumo Corp., Tokyo, Japan). Umbilical cord blood cells were collected after normal labor at the National Center for Child Health and Development. All blood samples were obtained with informed consent and were assayed within 24 hours. Specific interactions between lymphocytes and sugar-VP in the presence or absence of SBA were examined by flow cytometry with fluorescent anti-CD3 and sugar-VP–coated microbeads. To coat the microbeads with sugar-VP, 1 mL of fluorescent microbeads (diameter 0.5 μm, 10 ng/mL, Invitrogen Corp., Carlsbad, CA) was added to an equivalent volume of an aqueous solution of sugar-VP (200 μg/mL). After incubation at 4°C for at least 4 hours, the fluorescent beads were washed twice by centrifugation with PBS containing 0.1 percent sodium azide and 0.1 percent BSA and resuspended in 1 mL of PBS. Mononuclear cells (MNCs) were obtained from peripheral blood of healthy adults by density-gradient centrifugation with 1.077 g per mL Ficoll-Hypaque (Pharmacia, Uppsala, Sweden). The isolated cells (10^6 cells) were suspended in 1 mL of divalent cation-free PBS containing 0.1 percent sodium azide and 0.1 percent BSA and then incubated with PE-labeled anti-CD3 (Becton Dickinson Labware, Franklin Lakes, NJ) according to the manufacturer's instructions. After being washed with PBS, the cells were resuspended in PBS at a final density of 10^6 cells per mL. A 10-mL aliquot of the suspension of fluorescent beads and 10 mL of PBS containing SBA (1 mg/mL, SBA L-1010-010, Vector, Burlingame, CA) were added to 100 mL of the cell suspension and the mixture was incubated at 4°C for 30 minutes. Fluorescence intensities of the cells treated with the antibody and the fluorescent beads were measured by flow cytometry (FACScan, Becton Dickinson Immunocytometry Systems, San Jose, CA).[12]

The selectivity of SBA for blood cells was evaluated by testing cellular attachment to sugar-VP–coated plates. When cell culture plates were treated with 100 μg per mL aqueous sugar-VP for 2 hours, approximately 0.6 μg per cm^2 sugar-VP was immobilized on the plates. Cells from human peripheral blood or cord blood were collected as the mononuclear fraction after density-gradient centrifugation. The collected cells were suspended in PBS containing 0.1 percent (wt/vol) BSA and adjusted to a final concentration of 2×10^6 cells per mL. The proportion of adherent cells was calculated from the number of unattached cells after incubation at 37°C for 30 minutes in the presence of SBA. The phenotypes of T lymphocytes, natural killer (NK) cells, or hematopoietic stem cells were assessed by flow cytometry with fluorescent anti-CD3, anti-CD16, or anti-CD34 (Becton Dickinson Labware).

TABLE 1. Comparison of absorption of sugar-VPs or sugars to different materials

	Polystyrene	Polycarbonate	Polymethylpentene	Polymethylmethacrylate	Glass
Sugar-VPs					
α-1,6-Gal-VP	+++	+++	+++	+	++
β-1,4-Gal-VP	+++	+++	+++	+	++
α-1,4-Glu-VP	+++	+++	+++	+	++
Sugars					
Lactose	ND	–	–	ND	–
Galactose	ND	–	–	ND	–

RESULTS

Sugar-VPs (α-1,6-Gal-VP, β-1,4-Gal-VP, and α-1,4-Glu-VP) adsorbed well to the surfaces of various materials, whereas sugars (lactose and maltose) were not adsorbed (Table 1). α-1,6-Gal-VP gave the same adsorption profile as those of β-1,4-Gal-VP and α-1,4-Glu-VP (data not shown). Plates made of relatively hydrophilic materials, such as glass, required a higher concentration to obtain adequate adsorption of α-1,6-Gal-VP, compared with hydrophobic materials such as polystyrene (Fig. 3).

CD3+ T lymphocytes exhibited increased binding affinity for β-1,4-Gal-VP–coated microbeads in the presence of SBA (Figs. 4A and 4B). These cells, however, did not bind α-1,4-Glu-VP–coated microbeads in the presence (Fig. 4C) or absence (data not shown) of SBA. These findings indicate that the interaction between sugar-VP and SBA might be mediated by specific recognition of the galactose moiety on the microbeads. To determine the specificity of SBA for the sugar-VPs, we compared the adherent activities of peripheral blood MNCs (PBMNCs) on α-1,6-Gal-VP– and β-1,4-Gal-VP–coated plastic plates in the presence of SBA. The adherent activity of PBMNCs on α-1,6-Gal-VP–coated plates was higher than that on β-1,4-Gal-VP–coated plates at lower concentrations of SBA (Fig. 5). A previous report showed that SBA exhibits preferential binding affinity for α-linked galactose compared to β-linked galactose.[13] Cell attachment following SBA adherence reflects the specific recognition of sugar structures in Gal-VP.

The adherent activity of RBCs or PBMNCs to α-1,6-Gal-VP increased in a dose-dependent manner with respect to SBA and differed among cell lineages. T lymphocytes, NK cells, granulocytes-monocytes, and RBCs exhibited high adherent activity with α-1,6-Gal-VP–coated plates in the presence of SBA (300 mg/mL), whereas most CD34+ cells did not adhere, even in the presence of a higher concentration of SBA (800 mg/mL) (Table 2). These results suggest that α-1,6-Gal-VP–coated plates in combination with SBA can be used to separate blood cells and especially CD34+ hematopoietic stem cells.

TABLE 2. Selective adhesion of blood cells to α-1,6-Gal-VP–coated plates in the presence of SBA

Adherent activity of blood cells on α1,6-Gal-VP(%)				
+SBA (300 μg/ml)				+SBA (800 μg/ml)
T lymphocytes	NK cells	Granulocytes-monocytes	RBCs	CD34+ cells
85.4 ± 13.8	69.6 ± 22.3	100 ± 0	100 ± 0	20.8 ± 11.0

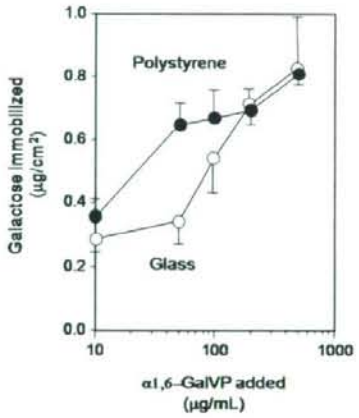

Fig. 3. Representative adsorption profile of α-1,6-Gal-VP on polystyrene (○) or glass (●) plates. Data points are means from assays performed in triplicate.

DISCUSSION

We synthesized a novel material that allows separation of hematopoietic stem cells with SBA, which has multiple binding sites for sugar residues.[1] Reisner and coworkers[9] succeeded in reducing the occurrence of GVHD after allograft transplantation through selective depletion of T lymphocytes by mixing a core of galactose-rich sheep RBCs with SBA. The sheep RBCs, however, were required for adhesion and separation, and this prevented satisfactory degrees of stability, safety, and utility.[14] For this reason, the sheep-RBC separation system has not become a standard technique. In this study, we used a core mate-

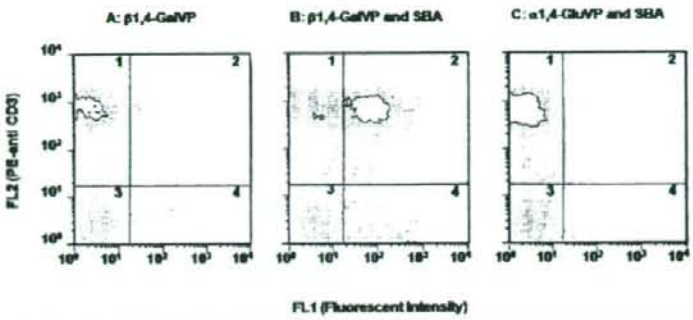

Fig. 4. PBMNCs were cultured with β-1,4-Gal-VP–coated microbeads in the presence (B) or absence (A) of SBA or α-1,4-Glu-VP–coated microbeads and SBA (C).

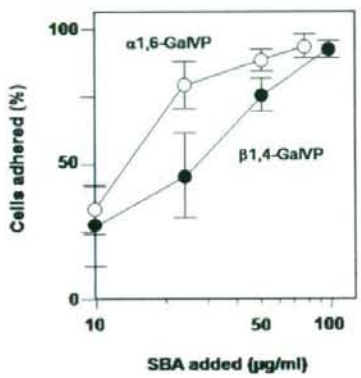

Fig. 5. Proportion of adherent cells on α-1,6-Gal-VP–coated (○) or β-1,4-Gal-VP–coated (●) plates. Data points are means from assays performed in triplicate.

rial with a modified sugar-VP–coated surface for adhesion and separation to overcome the limitations of lectin-mediated separation.

Gal-VPs synthesized from galactose and vinyl monomers can easily be modified to include sugar chains with α-1,4-Gal-VP or α-1,6-Gal-VP structures. Such modified polymers have similar physical properties, but exhibit distinct binding patterns based on the galactose residues. The sugar-VPs are able to coat and glycosylate the surface of various materials for medical use[15] and show preferential adherence to hydrophobic plastic materials such as polystyrenes.[16] Sugar-VPs include a hydrophobic VP unit and a hydrophilic sugar and have been shown to be effective for encapsulating and solubilizing insoluble pharmaceutical agents.[17] The preferential adsorption of a VP on hydrophobic materials such as polystyrene, polycarbonate, or polymethylpentene, rather than polymethylmethacrylate or glass, is due to the hydrophobic interaction between the polystyrene main chain of the VP and the solid support.

Coating of the surface of polystyrene microbeads with β-1,4-Gal-VP caused specific binding of the beads to T lymphocytes in the presence of the galactose-specific lectin, SBA. Moreover, these cells preferentially adhered to α-1,6-Gal-VP–coated culture plates in the presence of SBA. These findings indicate that α-1,6-Gal-VP is effective as a core material to selectively adhere to and separate blood cells in the presence of SBA and that the selectivity of α-1,6-Gal-VP is equivalent to that of monoclonal antibodies. The order of the adherent activity of blood cells for SBA was RBCs > granulocytes/monocytes > T lymphocytes > NK cells > hematopoietic stem cells. Expression of cell surface sugar chains depends on the stage of cell differentiation and the cell lineage,[8,18] and the results obtained from our system correlate remarkably well with the lack of expression of sugar chains on immature cells.

A recent study has shown that immunomagnetic bead systems impair the function of CD34+ cells.[19] Although SBA binds to marrow MNCs, however, including mature myeloid, erythroid, and lymphoid cells, it has very low binding affinity and no toxicity toward human hematopoietic cells.[8] SBA has also been used as a T-lymphocyte–depleting agent before CD34+ cell collection because of the absence of specific binding materials for SBA. Gal-VP makes it possible to remove CD34+ cells from marrow fluid without the use of expensive anti-CD34 and the polymer is easily mounted on various solid supports. Therefore, a cell separation system with Gal-VP and SBA may be advantageous for CD34+ cell collection from both clinical and economic perspectives.

REFERENCES

1. Weis WI, Drickamer K. Structural basis of lectin-carbohydrate recognition. Annu Rev Biochem 1996;65:441-73.
2. Rando RR, Orr GA, Bangerter FW. Threshold effects on the concanavalin A-mediated agglutination of modified erythrocytes. Biol Chem 1979;254:8318-23.
3. Paetkau V, Mills G, Gerhart S, Monticone V. Proliferation of murine thymic lymphocytes in vitro is mediated by the concanavalin A-induced release of a lymphokine (costimulator). J Immunol 1976;117:1320-4.
4. Basrur VS, Chitnis MP, Menon RS. Cell surface alterations in murine leukaemia P388 adriamycin-resistant cells: studies on lectin-induced agglutination and rearrangement of lectin receptors. Oncology 1985;42:328-31.
5. Kitagawa M, Sugiura K, Omi H, Akiyama Y, Kanayama K, Shinya M, Tanaka T, Yura H, Sago H. New technique using

galactose-specific lectin for isolation of fetal cells from maternal Blood. Prenat Diagn 2002;22:17-21.
6. Nagai K, Yamaguchi HJ. Direct demonstration of the essential role of the intramolecular high-mannose oligosaccharide chains in the folding and assembly of soybean (glycine max) lectin polypeptides. Biochem (Tokyo) 1993;113:123-5.
7. Tsuda M, Kurokawa T, Takeuchi M, Sugino Y. Changes in cell surface structure by viral transformation studied by binding of lectins differing in sugar specificity. Gann 1975; 66:513-21.
8. Nagler A, Morecki S, Slavin S. The use of soybean agglutinin (SBA) for bone marrow (BM) purging and hematopoietic progenitor cell enrichment in clinical bone-marrow transplantation. Mol Biotechnol 1999;11:181-94.
9. Reisner Y, Kapoor N, Hodes MZ, O'Reilly RJ, Good RA. Enrichment for CFU-C from murine and human bone marrow using soybean agglutinin. Blood 1982;59: 360-3.
10. Schain LR, Okrongly D, Okarma TB, Lebkowski JS. Separation of lectin-binding cells using polystyrene culture devices with covalently immobilized soybean agglutinin. J Hematother 1994;3:37-46.
11. Yura H, Goto M, Okazaki H, Kobayashi K, Akaike T. Structural effect of galactose residues in synthetic glucoconjugates on interaction with rat hepatocytes. J Biomed Mater Res 1995;29:1557-65.
12. Kanatani Y, Kasukabe T, Okabe-Kado J, Hayashi S, Yamamoto-Yamaguchi Y, Motoyoshi K, Nagata N, Honma Y. Transforming growth factor beta and dexamethasone cooperatively enhance c-jun gene expression and inhibit the growth of human monocytoid leukemia cells. Cell Growth Differ 1996;7:187-96.
13. Rao VS, Lam K, Qasba PK. Three dimensional structure of the soybean agglutinin Gal/GalNAc complexes by homology modeling. J Biomol Struct Dyn 1998;15:853-60.
14. Meijer E, Slaper-Cortenbach IC, Thijsen SF, Dekker AW, Verdonck LF. Increased incidence of EBV-associated lymphoproliferative disorders after allogeneic stem cell transplantation from matched unrelated donors due to a change of T cell depletion technique. Bone Marrow Transplant 2002;29:335-9.
15. Satoh A, Kojima K, Koyama T, Ogawa H, Matsumoto I. Immobilization of saccharides and peptides on 96-well microtiter plates coated with methyl vinyl ether-maleic anhydride copolymer. Anal Biochem 1998;260:96-102.
16. Suzuki N, Quesenberry MS, Wang JK, Lee RT, Kobayashi K, Lee YC. Efficient immobilization of proteins by modification of plate surface with polystyrene derivatives. Anal Biochem 1997;247:412-6.
17. Sheorey DS, Sai MS, Dorle AK. A new technique for the encapsulation of water insoluble drugs using ethyl cellulose. J Microencapsul 1991;8:359-68.
18. Gengozian N, Reyes L, Pu R, Homer BL, Bova FJ, Yamamoto JK. Fractionation of feline bone marrow with the soybean agglutinin lectin yields populations enriched for erythroid and myeloid elements: transplantation of soybean agglutinin-negative cells into lethally irradiated recipients. Transplantation 1997;64:510-8.
19. Kimura T, Minamiguchi H, Wang J, Kaneko H, Nakagawa H, Fujii H, Sonoda Y. Impaired stem cell function of CD34+ cells selected by two different immunomagnetic beads systems. Leukemia 2004;18:566-74. ■

Accelerated Wound Healing in Healing-Impaired *db/db* Mice by Autologous Adipose Tissue-Derived Stromal Cells Combined With Atelocollagen Matrix

Masaki Nambu, MD, Satoko Kishimoto, DVM,† Shingo Nakamura, PhD,‡ Hiroshi Mizuno, MD, PhD,§ Satoshi Yanagibayashi, MD,* Naoto Yamamoto, MD, PhD,* Ryuichi Azuma, MD,* Shin-ichiro Nakamura, MD,* Tomoharu Kiyosawa, MD, PhD,* Masayuki Ishihara, PhD,† and Yasuhiro Kanatani, MD, PhD†*

Abstract: Adipose tissue-derived stromal cells (ATSCs) have recently gained widespread attention as a potential alternate source to bone marrow–derived mesenchymal stem cells with a proliferative capacity and a similar ability to undergo multilineage differentiation. In this study, we evaluated the effectiveness of freshly isolated autologous ATSCs-containing atelocollagen matrix with silicon membrane (ACMS) on wound healing of diabetic (*db/db*) mice.

Cultured ATSCs from (*db/db*) mice secreted significant amounts of growth factors and cytokines, which are suitable for wound repair. Two full thickness round skin defects were made on the backs of healing-impaired *db/db* mice. Freshly isolated autologous ATSCs-containing ACMS or ACMS alone were applied to the wounds. Twelve mice were treated and then killed at 1 or 2 weeks (n = 6 each). Histologic sections of the wounds were prepared at each time period after treatment.

Histologic examination demonstrated significantly advanced granulation tissue formation, capillary formation, and epithelialization in diabetic healing-impaired wounds treated with autologous ATSCs-containing ACMS, compared with mice treated with ACMS alone. These results suggested that transplantation of autologous ATSCs-containing ACMS significantly accelerated wound healing in diabetic healing-impaired *db/db* mice.

Key Words: wound healing, adipose tissue-derived stromal cells, *db/db* mice

(*Ann Plast Surg* 2009;62: 317–321)

Lack of cellular and molecular signals required for normal wound repair processes, such as inflammation, angiogenesis, contraction, deposition of extracellular matrix, granulation tissue formation, epithelialization, and remodeling, may be major contributing factors to poor healing of some wounds such as diabetic ulcers.[1] Numerous strategies for coverage of such skin defects, including temporary substitutes (porcine xenografts, synthetic membranes, atelocollagen sponge, allogenic substitutes) and permanent skin substitutes (cultured epidermis and dermal substitutes), have been investigated.[2,3] Among them, artificial dermal substitutes, such as atelocollagen matrix with silicon membrane (atelocollagen matrix with silicon membrane [ACMS]; PELNAC; Johnson & Johnson, Tokyo, Japan), are structurally optimized to incorporate into surrounding tissue and to allow cell invasion by fibroblasts and capillaries for subsequent dermal remodeling.[3,4] Nevertheless, effective skin coverage is still not established when the area is large or the local condition of the recipient is poor, such as severe contamination, excessively poor blood flow and vascularity, or for congenital skin disorders such as epidermolysis bullosa.[3,5]

Mesenchymal stem cells have recently received widespread attention because of their potential utility in wound repair and tissue-engineering applications. Bone marrow-derived mesenchymal stem cells are multipotent[6] in that they differentiate in culture[7] or after implantation in vivo into many different cell types, including osteoblasts,[6] chondrocytes,[8] adipocytes,[9] myotubes,[10] and neuronal cells.[11] Although it is known that many tissues contain lineage-committed progenitor cells for tissue maintenance and repair, several studies have demonstrated the presence of uncommitted progenitor cells within the matrix of connective tissues.[12] For instance, human adipose tissue-derived multilineage (stromal) cells have the potential to differentiate into bone,[13] cartilage,[14] fat,[15] myocardium,[16] skin,[17] skeletal muscle,[18] and neurons.[19,20] No significant differences were observed between adipose tissue-derived stromal cells (ATSCs)and human bone marrow-derived mesenchymal stem cells (BMSCs) from the same patient for yield of adherent cells, growth kinetics, cell senescence, differentiation capacity, or gene transduction efficiency.[21] Furthermore, it has been reported that transplantation of human ATSCs-cultured constructs significantly stimulated skin repair, angiogenesis, and re-epithelialization in athymic mice when compared with human fibroblast-cultured constructs.[22] The multipotent characteristics of ATSCs, as well as their abundance in the human body, make these cells a potential source in wound repair and tissue engineering applications.

A previous wound healing study using a mitomycin C-treated, healing-impaired rat model has shown that application of inbred ATSCs-containing ACMS onto an open wound significantly induced granulation tissue and capillary formation, and accelerated wound healing.[23] To further evaluate the effectiveness of autologous ATSCs-containing ACMS, full thickness skin incisions were made on the backs of healing-impaired diabetic (*db/db*) mice. The present study demonstrated advanced granulation tissue formation, capillary formation, and epithelialization in wounds applied with autologous ATSCs-containing ACMS. Because of its ability to accelerate wound healing, autologous ATSCs-containing ACMS may become accepted as a wound dressing for healing-impaired wound management.

MATERIALS AND METHODS

Isolation of ATSCs From Adipose Tissue of *db/db* Mice

Male mutant diabetic mice, C57BL/ksJ *db/db* (CREA Japan Inc, Tokyo, Japan) were used in this study. All mice were main-

Received October 4, 2007, and accepted for publication, after revision, May 6, 2008.

From the *Department of Plastic and Reconstructive Surgery, †Research Institute, and ‡Department of Surgery II, National Defense Medical College, Saitama, Japan; and the §Department of Plastic and Reconstructive Surgery, Nippon Medical School, Tokyo, Japan.

Reprints: Yasuhiro Kanatani, PhD, MD, Research Institute, National Defense Medical College, 3-2 Namiki, Tokorozawa, Saitama, 359-8513 Japan. E-mail: ykanatan@ndmc.ac.jp.

ISSN: 0148-7043/09/6203-0317
DOI: 10.1097/SAP.0b013e31817f01b6

tained on a standard laboratory diet and water ad libitum, and were used experimentally when older than 10 weeks of age. Before the start of the experiments, urinary glucose and protein were analyzed using reagent strips (Uro-Labstrix, Bayer Medical Ltd, Tokyo, Japan), and all of the *db/db* mice were diagnosed as severely diabetic.

Adipose tissue was obtained from the abdomen of *db/db* mice. ATSCs were prepared as described previously.[13,14,23] Briefly, approximately 1 g of adipose tissue obtained from 1 *db/db* mouse was washed extensively with 10 mL of phosphate-buffered saline, and extracellular matrix was digested with 0.075% collagenase at 37°C for 1 hour. After adding Dulbecco Modified Eagle Medium containing 10% fetal bovine serum and antibiotics (control medium), samples were centrifuged at 1200*g* for 10 minutes. The cell pellet was resuspended in medium and incubated at room temperature for 10 minutes. After removing cellular remains through a 100-μm Nylon mesh, the cells were resuspended with control medium and about 5×10^5 cells were plated into round ACMS (1.5 cm in diameter; PELNAC, Gunze Corp, Kyoto, Japan). ATSCs-containing ACMS were incubated in control medium at 37°C for 2 hours before transplantation. The yield of adhered cells (ATSCs) was estimated to be about $4–6 \times 10^5$ cells per 1 g of adipose tissue obtained from 1 *db/db* mouse.

Transplantation of ATSCs-Containing ACMS

Under general anesthesia using pentobarbital sodium (Dainippon Sumitomo Pharma Co, Ltd, Osaka, Japan), the dorsal area was totally depilated and 2 full thickness round wounds (approximately 1.5 cm in diameter) were created on the back of each *db/db* mouse using a pair of sharp scissors and a scalpel. A freshly isolated ATSCs-containing ACMS, or ACMS alone (control), were applied to the wound by suture using 6-O nylon sutures (Kono Seisakusho Co, Ltd, Chiba, Japan) (Fig. 1). The skin including the wound was removed from each *db/db* mouse for histologic examination at 1 (Fig. 2) and 2 weeks (Fig. 3) posttreatment (n = 6 each). These animal experiments were approved and carried out following the guidelines for animal experimentation of the National Defense Medical College, Tokorozawa, Saitama, Japan.

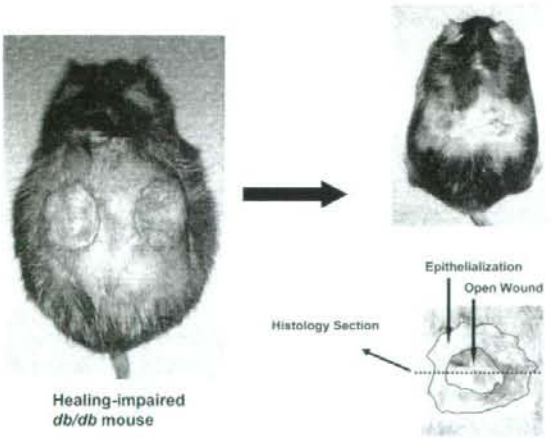

FIGURE 1. ATSCs-containing ACMS or ACMS only (control) was applied to the wound by suture. After silicon membranes were removed, skin including wounds was removed and sectioned for histologic examination. Sections were made perpendicular to the wound surface.

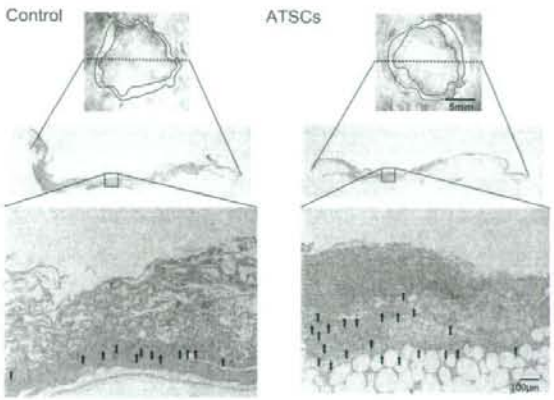

FIGURE 2. Histologic examination of wound repair of ATSCs-containing ACMS and ACMS only (control) wounds at 1 week after initial wounding. Photographs are representative of 6 ATSCs-containing ACMS or control wounds stained with H&E (second and third panels). Arrows show mature blood vessels containing erythrocytes.

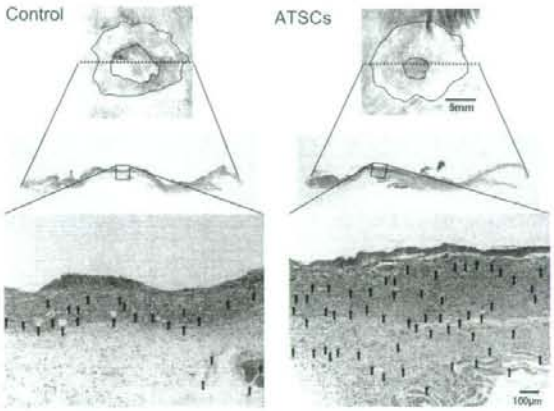

FIGURE 3. Histologic examination of wound repair of ATSCs-containing ACMS and ACMS only (control) wounds at 2 weeks after initial wounding. Photographs are representative of 6 ATSCs-containing ACMS or control wounds stained with H&E (second and third panels). Arrows show blood vessels containing erythrocytes.

Histologic Examination

Removed skins including wound tissue were fixed in a 10% formaldehyde solution, embedded in paraffin and sectioned in 4-μm increments (Yamato Kohki Inc, Asaka, Saitama, Japan). Sections were made perpendicular to the anterior-posterior axis and perpendicular to the surface of the wound. Sections were stained with hematoxylin-eosin (H&E) reagent (Figs. 2, 3). For each section, a randomized area (magnification, 100×) showing granulation and capillary formation was photographed, and the thickness of granulation formation and number of capillary lumens per microphotograph was evaluated (Figs. 4, 5). Only mature vessels containing erythrocytes were counted.

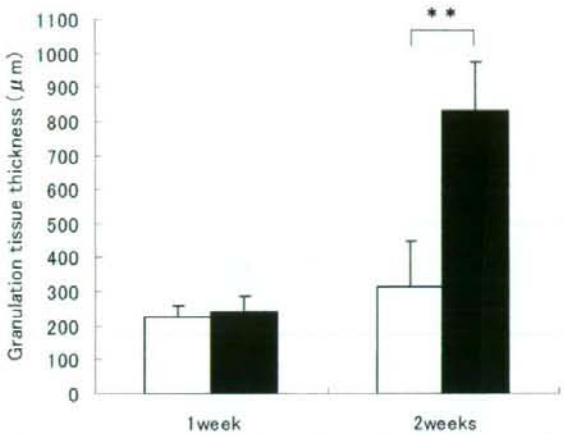

FIGURE 4. In both ATSC-containing ACMS (black bars) and control (white bars) wounds, a randomized area (magnification, 100×) showing granulation at weeks 1 and 2 was photographed (third panels in Figs. 2 and 3), and the thickness of granulation formation per microphotograph was evaluated. Data represent the mean ± SD of 6 determinations. **Student t test, $P < 0.005$.

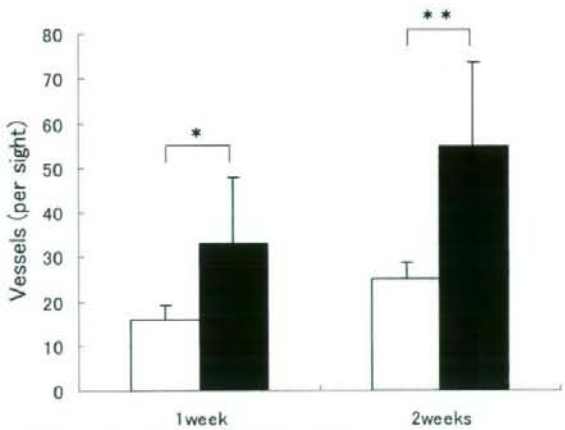

FIGURE 5. In both ATSC-containing ACMS (black bars) and control (white bars) wounds, a randomized area (magnification 100×) showing capillary formation at weeks 1 and 2 was photographed (third panels in Figs. 2 and 3), and the number of capillary lumens per microphotograph was evaluated. Data represent the mean ± SD of 6 determinations. *Student t test, $P < 0.05$. **Student t test, $P < 0.005$.

Wound Closure Analysis

Digital photographs were taken 1 and 2 weeks after the silicon membrane was removed. The silicone membranes of half of the animals were removed after 1 week and the silicone membranes of other half of the animals were removed after 2 weeks. Wound closure was quantified by epithelialization rates (Fig. 1). Epithelialization rates (%) were calculated by the equation "(1 − open wound area/original wound area) × 100" (Table 1).

TABLE 1. Epithelialization Rate (%)

	Control	ATSCs
1 wk	12.9 ± 8.8	19.8 ± 9.8
2 wk	57.8 ± 12.9	87.3 ± 5.1*

Epithelialization rates (%) were calculated by the equation "(1 − open wound area/original wound area) ± 100": Data represent mean ± SD.
*Student t test, $P < 0.05$.

Growth Factor and Cytokine Quantification

ATSCs (1×10^6) were plated on 10-cm diameter plastic dishes. ATSC-conditioned medium was collected 4 and 8 days after plating. At the end of the culture period, supernatants were collected and stored at −80°C until analysis. The presence of cytokines was analyzed using the BioPlex system (Bio-Rad Laboratories Co, Ltd, Tokyo, Japan). The following cytokines were analyzed: interleukin 6, granulocyte colony-stimulating factor, granulocyte-macrophage colony-stimulating factor, macrophage colony-stimulating factor, basic fibroblast growth factor (b-FGF), platelet-derived growth factor bb (PDGF-bb), and vascular endothelial growth factor (VEGF). Hepatocyte growth factor (HGF) levels in cell culture supernatants were measured using an ELISA kit (Institute of Immunology Co, Ltd, Tokyo, Japan).

Statistical Analysis

Results are expressed as means ± SD. A paired Student t test was used to determine the probability of significant differences. A value of $P < 0.05$ was considered to be statistically significant.

RESULTS

Gross Observations

No sign of undesirable inflammation, infection, neovascularization, or adipose tissue formation was observed in ATSCs-containing ACMS-treated wounds. After the silicon membrane was removed at 7 days, wound areas were recorded with the aid of a digital camera. Because the presence of the silicon membrane in ACMS negatively blocked the migration of keratinocytes, we did not observe significant stimulation of epithelialization during the first week (Fig. 2 and Table 1). However, the wound at 2 weeks significantly enhanced re-epithelialization during wound healing compared with control wounds (Fig. 3 and Table 1).

Granulation Tissue Thickness

Only minor stimulation of granulation was observed in the ATSCs-containing ACMS at 1 week. However, significant stimulatory effects were shown on granulation in the ATSCs-containing ACMS at 2 weeks.

Capillary Number

Significant stimulatory effects on capillary formation were demonstrated in the ATSCs-containing ACMS wounds both at 1 and 2 weeks (Fig. 5). Only minor effects on capillary formation were observed in ACMS-treated control wounds.

Growth Factor and Cytokine Quantification

Cultured ATSCs from *db/db* mice secreted significant amounts of growth factors and cytokines such as interleukin 6, b-FGF, PDGF-bb, VEGF, and HGF at 4 and 8 days (Fig. 6). Generation of growth factors might be suitable for regenerative ATSC therapy in the healing-impaired wound.

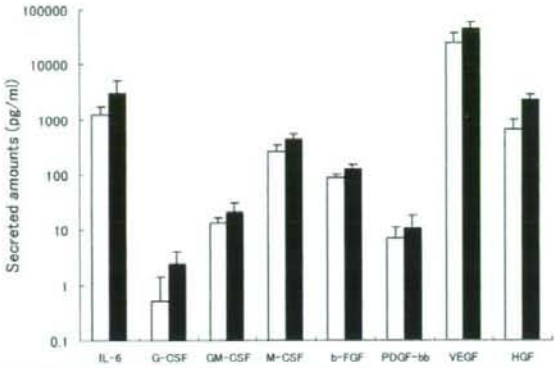

FIGURE 6. Growth factors and cytokines present in cell culture supernatants were analyzed on day 4 (white bars) and day 8 (black bars). Data represent the mean ± SD of duplicate samples from 3 culture supernatants. **Student *t* test, $P < 0.005$.

C57BL/ksJ (*db/+*) Mice

The effects of ATSCs-containing ACMS, or ACMS alone, were also assessed in the wounds of C57BL/ksJ (*db/+*) mice, the normal heterozygous littermates of *db/db* mice (CREA Japan Inc, Tokyo, Japan). No statistically significant differences between treatments were observed throughout the entire study period regarding granulation, epithelium, and capillary formation (data not shown). Thus, the introduction of ATSCs into ACMS had little stimulatory effect on normal wound healing.

DISCUSSION

It is well known that many adult tissues contain lineage-committed progenitor cells for tissue maintenance and repair. Mesenchymal stem cells derived from bone marrow have been shown to be multipotent in that they differentiate in culture[6] or after implantation in vivo.[7–10] Similarly, we and others previously reported that adipose tissue-derived stromal cells (ATSCs) isolated from adipose tissue possess the ability to produce cartilage and bone matrix.[12–14] In this study, we showed that freshly isolated, undifferentiated autologous ATSCs-containing ACMS can enhance formation of granulation tissue, epithelium, and vascularization in full thickness wounds of healing-impaired diabetic (*db/db*) mice and can contribute to dermal regeneration. This finding demonstrates that ATSCs seeded in ACMS may provide a novel and abundant autologous cell source for developing tissue-engineering approaches to repair healing-impaired, deep, and chronic wounds.

Wound healing proceeds in 3 overlapping phases, namely (i) inflammation, (ii) proliferation, including granulation tissue formation, and (iii) matrix formation and remodeling.[24] This sequential process requires interaction of cells in the dermis and epidermis, as well as release of chemical mediators from inflammatory cells, fibroblasts and keratinocytes. Proliferation of mesenchymal cells and capillaries, as well as the influx of macrophages into granulation tissue, serves to replace lost dermis and to provide substrates and inducers for re-epithelialization. Although the mechanism responsible for impaired wound healing in *db/db* mice is not completely understood, it is likely that the presence of macrophages has a significant effect on the formation of wound granulation tissue, and that macrophage accumulation is impaired in *db/db* mice.[24] Furthermore, a defect in vascular endothelial growth factor expression may be associated with any wound-healing disorder.[25]

We used noncultured, autologous ATSCs-containing ACMS to enhance wound healing of *db/db* mice in this study. ATSCs-containing ACMS has potential advantages over other cellular dermal substitutes for clinical use. Large quantities of ATSCs could be obtained from human adipose tissue by liposuction under local anesthesia, so cell multiplication under expensive and laborious cell-culture conditions would not be required. Approximately 5×10^5 cells per 1 g of adipose tissue could be obtained from human adipose tissue by liposuction (data not shown). In contrast to a cultured dermal substitute, our ATSCs-containing ACMS can be prepared within a few hours in a clinical setting. Furthermore, our ATSCs-containing ACMS allows the use of autologous cells (ATSCs), which prevents risks of transmitting infectious diseases and cellular rejections.

When ACMS alone was applied to an open wound in *db/db* mice, minor effects were demonstrated on granulation tissue formation, epithelialization, and capillary number. However, parameters such as granulation tissue thickness, epithelium, and vessel formation were significantly increased in the autologous ATSCs-containing ACMS-treated wounds at 1 or 2 weeks in the *db/db* mice. Thus, the addition of autologous ATSCs to ACMS enhanced granulation tissue, epithelium, and capillary formation in healing-impaired wounds. Interestingly, cultured ATSCs secreted a number of angiogenic cytokines such as b-FGF, PDGF-bb, VEGF, and HGF at levels that are bioactive (Fig. 6). Introduced ATSCs in vivo could also up-regulate expression of these growth factors by autocrine and/or paracrine actions in the wound. However, the fate of the seeded autologous ATSCs into healing-impaired wounds, differentiation of autologous ATSCs, and interactions between seeded autologous ATSCs and their environment are subjects of further investigation. Preliminary experiments indicate that the majority of seeded autologous ATSCs incorporate into the regenerated granulation tissues.

It is interesting to note that addition of autologous ATSCs into ACMS had only minor effects on the degree of healing in normal (*db/+*) mice (data not shown). Although the mechanism responsible for this is not completely understood, it is likely that the presence of macrophages has a significant effect on the formation of wound granulation tissue,[24] and that enough macrophages accumulate in *db/+* mice. Thus, it is possible that *db/+* mice have a sufficient amount of growth factors in the wound and wound fluid to achieve a maximal rate of healing, and therefore only a minor increase in wound repair is possible upon application of autologous ATSCs. On the other hand, the wound closure assay and histologic examinations used in this study might not be sensitive enough to detect small effects.

In conclusion, although the mechanism responsible for impaired wound healing in *db/db* mice is not completely understood, wound healing experiments using the *db/db* mouse model have shown that application of autologous ATSCs-containing ACMS onto an open wound induced significant granulation tissue, epithelium, and capillary formations, which accelerated wound healing.

REFERENCES

1. Robson MG, Hill DP, Smith PD, et al. Sequential cytokine therapy for pressure ulcer: clinical and mechanistic response. *Ann Surg*. 2000;231:600–611.
2. Sheridan RL, Tompkins RG. Skin substitutes in burns. *Burns*. 1999;25:97–103.
3. Nakagawa H, Akita S, Fukui M, et al. Human mesenchymal stem cells successfully improve skin-substitute wound healing. *Br J Dermatol*. 2005;153:29–36.
4. Suzuki S, Matsuda K, Isshiki N, et al. Experimental study of a newly developed bilayer artificial skin. *Biomaterials*. 1990;11:356–360.
5. Ortiz-Urda S, Lin Q, Green CL, et al. Injection of genetically engineered fibroblasts corrects regenerated human epidermolysis bullosa skin tissue. *J Clin Invest*. 2003;111:251–255.

6. Boo JS, Yamada Y, Okazaki Y, et al. Tissue-engineered bone using mesenchymal stem cells and biodegradable scaffold. *J Craniofac Surg*. 2002;13: 231–239.
7. Pittenger MF, Mackay AM, Beck SC, et al. Multilineage potential of adult human mesenchymal stem cells. *Science*. 1999;284:143–147.
8. Wakitani S, Goto T, Pineda SJ, et al. Mesenchymal cell-based repair of large, full-thickness defects of articular cartilage. *J Bone Joint Surg Am*. 1994;76: 579–592.
9. Beresford JN, Bennett JH, Devlin C, et al. Evidence for inverse relationship between the differentiation of adipocytic and osteogenic cells in rat marrow stromal cell cultures. *J Cell Sci*. 1992;102:341–351.
10. Ferrari G, Cusella-DeAngelis G, Coletta M, et al. Muscle regeneration by bone marrow-derived myogenic progenitors. *Science*. 1998;279:1528–1530.
11. Woodbury D, Reynoldsk B, Black IB. Adult bone marrow stromal stem cells express germline, ectodermal, endodermal, and mesodermal genes prior to neurogenesis. *J Neurosci Res*. 2002;69:908–917.
12. Zuk PA, Zhu M, Mizuno H, et al. Multilineage cells from human adipose tissue: implications for cell-based therapies. *Tissue Eng*. 2001;7:211–228.
13. Hattori H, Masuoka K, Sato M, et al. Bone formation using human adipose tissue-derived stromal cells and a biodegradable scaffold. *J Biomed Mater Res B Appl Biomater*. 2006;76:230–239.
14. Masuoka K, Asazuma T, Hattori H, et al. Tissue engineering of articular cartilage with autologous cultured adipose tissue-derived stromal cells using atelocollagen honeycomb-shaped scaffold with a membrane sealing in rabbits. *J Biomed Mater Res B Appl Biomater*. 2006;79:25–34.
15. Toriyama K, Kawaguchi N, Kitoh J, et al. Endogenous adipocyte precursor cells for regenerative soft-tissue engineering. *Tissue Eng*. 2002;8:157–165.
16. Miyahara Y, Nagaya N, Kataoka M, et al. Monolayered mesenchymal stem cells repair scarred myocardium after myocardial infarction. *Nature Med*. 12:459465, 2006.
17. Bogaerdt AJ, Zuijlen PP, Galen M, et al. The suitability of cells from different tissues for use in tissue-engineered skin substitutes. *Arch Dermatol Res*. 2002;294:135–142.
18. Mizuno H, Zuk PA, Zhu M, et al. Myogenic differentiation by human processed lipoaspirate cells. *Plust Reconstr Surg*. 2002;109:199–209.
19. Safford KM, Hicok KC, Safford SD, et al. Neurogenic differentiation of murine and human adipose-derived stromal cells. *Biochem Biophys Res Commun*. 2002;294:371–379.
20. Ashjian PH, Elbarbary AS, Edmonds B, et al. In vitro differentiation of human processed lipoaspirate cells into early neural progenitors. *Plast Reconstr Surg*. 2003;111:1922–1931.
21. De Ugarte DA, Morizono K, Elbarbary A, et al. Comparison of multi-lineage cells from human adipose tissue and bone marrow. *Cells Tissues Organs*. 2003;174:101–109.
22. Wang HJ, Pieper J, Schotel R, et al. Stimulation of skin repair is dependent on fibroblast source and presence of extracellular matrix. *Tissue Eng*. 2004; 10:1054–1064.
23. Nambu M, Ishihara M, Nakamura S, et al. Enhanced healing of mitomycin C-treated wounds in rats using inbred adipose tissue-derived stromal cells within an atelocollagen matrix. *Wound Repair Regen*. 2007;15:505–510.
24. Tsuboi R, Rifkin DB. Recombinant basic fibroblast growth factor stimulates wound healing in healing-impaired *db/db* mice. *J Exp Med*. 1990;172:245–251.
25. Frank S, Hubner G, Breier G, et al. Regulation of vascular endothelial growth factor expression in cultured keratinocytes. Implications for normal and impaired wound healing. *J Biol Chem*. 1995;270:12607–12613.

MOLECULAR REPRODUCTION AND DEVELOPMENT 75:1085–1093 (2008)

Cre-*loxP* System as a Versatile Tool for Conferring Increased Levels of Tissue-Specific Gene Expression From a Weak Promoter

SHINGO NAKAMURA,[1] SATOSHI WATANABE,[2] MASATO OHTSUKA,[3] TADAAKI MAEHARA,[1] MASAYUKI ISHIHARA,[4] TAKAAKI YOKOMINE,[5] AND MASAHIRO SATO[6]*

[1]*Department of Surgery, School of Medicine, National Defense Medical College, 3-2 Namiki, Tokorozawa, Saitama, Japan*
[2]*Animal Genome Research Unit, Division of Animal Science, National Institute of Agrobiological Sciences, 2 Ikenodai, Tsukuba, Ibaraki, Japan*
[3]*Division of Basic Molecular Science and Molecular Medicine, School of Medicine, Tokai University, Bohseidai, Isehara, Kanagawa, Japan*
[4]*Division of Biomedical Engineering, The Research Institute, National Defense Medical College, 3-2 Namiki, Tokorozawa, Saitama, Japan*
[5]*Laboratory of Frontier Medicine, Frontier Science Research Center, 8-35-1 Sakuragaoka, Kagoshima, Kagoshima, Japan*
[6]*Section of Gene Expression Regulation, Frontier Science Research Center, Kagoshima University, 1-21-40 Kohrimoto, Kagoshima, Kagoshima, Japan*

ABSTRACT Attempts to image reporter gene expression driven by weak promoters are often hampered by the poor transcriptional activity of such promoters. Most tissue-specific promoters are weak compared with stronger but constitutively expressing viral promoters. In this study, we validated methods of enhancing the transcriptional activity of weak promoters using a Cre-*loxP* system in vitro and in vivo. We constructed a tester vector, pCTL, which carries a strong systemic cytomegalovirus enhancer/chicken β-actin promoter (CAG), *loxP*-flanked CAT, and firefly luciferase (luc) cDNAs. Herpes simplex virus-thymidine kinase (HSV-*tk*) promoter was used as a weak and systemic promoter and ligated to Cre for construction of pTC. Luc activity was higher (about 10-fold enhancement) in co-transfected (with pCTL and pTC) than in singly (with HSV-*tk* promoter-driven luc expression vector pTL) transfected NIH3T3 cells. In vivo electroporation-mediated gene delivery of both pCTL and pTC into murine oviductal epithelium yielded results (about 16-fold enhancement) similar to those obtained with in vitro-transfected NIH3T3 cells. To evaluate tissue-specific enhancement of gene expression, podocyte (glomerular visceral epithelial cell)-specific nephrin promoter was ligated to the Cre gene or luc cDNA to create pNC and pNL, respectively. We achieved 2.4-fold improvement of luc gene expression in the mouse kidney in vivo when pCTL and pNC were co-transfected via the tail vein via the lipoplex method. The combination of a weak tissue-specific promoter with the Cre-*loxP* system could thus be used to enhance the strength of tissue-specific promoters in vitro and in vivo. *Mol. Reprod. Dev. 75: 1085–1093, 2008.*

Key Words: Cre-*loxP* system; EGFP; fluorescent protein; weak promoter; luciferase; liposome; electroporation

INTRODUCTION

Targeted gene expression mediated by cell-type-specific promoters is one of the current challenges in the fields of gene therapy, transgenesis, cell trafficking, and regenerative medicine. A significant challenge for successful studies in these fields is to achieve high levels of expression of therapeutic genes confined to specific cell types; however, most tissue-specific promoters are weak compared to those derived from stronger but constitutively expressing viral promoters.

Several approaches have been developed to improve the transcriptional activity of weak promoters. For example, Nettelbeck et al. (1998) reported a novel strategy, termed "positive feedback loop", which is initiated by transcription from a cell-specific promoter. This is achieved by using a cell-type-specific promoter to drive simultaneous expression of the desired effector/reporter gene product and a strong artificial transcriptional activator [i.e., VP16 (viral

Grant sponsor: Ministry of Education, Science, Sports, Culture, and Technology of Japan; Grant number: 17100007; Grant sponsor: Research on Health Sciences focusing on Drug Innovation (Japan).

*Correspondence to: Dr. Masahiro Sato, The Section of Gene Expression Regulation, Frontier Science Research Center, Kagoshima University, 1-21-40 Kohrimoto, Kagoshima, Kagoshima 890-0065, Japan. E-mail: masasato@ms.kagoshima-u.ac.jp

Received 27 July 2007; Accepted 2 September 2007
Published online 28 December 2007 in Wiley InterScience (www.interscience.wiley.com).
DOI 10.1002/mrd.20847

transactivator)/LexA fusion transactivation factor]. This transcriptional activator in turn stimulates transcription through binding sites such as that for VP16/LexA fusion protein in the promoter. Using this method, they achieved from 14-fold to >100-fold enhancement of expression of a target protein. Iyer et al. (2001) developed a method similar to that of Nettelbeck et al. (1998), termed the "two-step amplification (TSTA) system", which can simultaneously amplify expression of both a target gene and a reporter gene, using a relatively weak promoter and GAL4-VP16 system. Since their report, evidence for augmentation of tissue-specific gene expression using TSTA-based systems has been provided by others (Emiliusen et al., 2001; Koch et al., 2001; Sato et al., 2003; Iyer et al., 2004, 2005; Ray et al., 2004; Lee et al., 2006; Liu et al., 2006; Dzojic et al., 2007). The use of small regulatory elements such as splice-signals (Brinster et al., 1988; Choi et al., 1991), serum response factor (SRF) sequence (Li et al., 1999, 2004), or the wood chuck hepatitis virus post-transcriptional regulatory element (WPRE) (Glover et al., 2002, 2003; Hermening et al., 2004) in combination with tissue-specific but weak promoters is known to elicit enhanced transgene expression. The latter two approaches have, however, only been used in viral vector systems.

Kaczmarczyk and Green (2001) first developed a Cre-*loxP*-based method for enhancement of tissue-specific gene expression. They constructed a single vector in which an expression unit containing a relatively weak but tissue-specific promoter + Cre recombinase gene had been linked to another expression unit containing a very strong promoter + *loxP*-flanked sequence (stopper) + a target gene of interest. By transfection of this vector into cultured cells, high levels of gene expression (300-fold amplification) from the tissue-specific promoter could be achieved as a result of Cre-induced transcriptional activation. Although this system appears to be relatively simple and basically effective for augmentation of the strength of a weak promoter, construction of a single vector into which all components related to the Cre-*loxP* system are included appears to be laborious and time-consuming. Furthermore, Kaczmarczyk and Green (2001) did not demonstrate the effectiveness of their system in vivo.

In this study, we intended to extend the work of Kaczmarczyk and Green (2001) with a co-transfection approach. The advantage of this approach is that it does not require construction of a single vector in which all the necessary materials must be included for Cre-mediated gene expression. Furthermore, the target gene can be expressed in any tissue desired, if a vector carrying the systemic and strong promoter, *loxP*-flanked sequence and a target gene is transfected in combination with a construct carrying a Cre gene linked to the upstream tissue-specific promoter. We validated the Cre-*loxP*-based co-transfection approach in vitro and in vivo, and found that this approach is adequate for enhancement of a weak tissue-specific promoter.

MATERIALS AND METHODS

Construction of Vectors

Nine constructs with three different promoters were constructed with the pBluescript SK(−) plasmid backbone (Stratagene, LaJola, CA) (Fig. 1A). The reporter plasmids, pCTL and pCTE, were constructed by replacing the 3-kb lacZ gene in pCAG-CAT-Z (Araki et al., 1995) with a 2.7-kb luciferase (luc) cDNA isolated from pMAMneo-LUC (CLONTECH Laboratories, Inc., Palo Alto, CA) and 0.9-kb enhanced green fluorescent protein (EGFP) cDNA (CLONTECH Laboratories, Inc.), respectively. pTC was constructed by combining 0.3-kb herpes simplex virus-thymidine kinase (HSV-*tk*) promoter (isolated by digestion with *Eco* RI and *Hin* dIII from p396/21-5 [Sato et al., 1993]) with the 1.5-kb NCre gene (carrying nuclear location signal in the region of the 5′ end of the Cre gene) isolated from pMBP/NCre (Sato et al., 1999). It was used as a positive vector for expression of Cre. pNC (=pTK174, kindly provided by Dr. Taiji Matsuzaka, Tokai University, School of Medicine, Japan) was constructed by ligating a ca. 5-kb fragment containing mouse nephrin promoter region and the 1st intron and a portion of the 1st exon to the NCre gene. The size of the nephrin promoter is almost the same as shown by Moeller et al. (2000) who reported that this promoter region conferred podocyte (glomerular visceral epithelial cell)-specific expression of a target gene in the transgenic mice. pNL was constructed by replacing the NCre gene in pNC by luc cDNA. pTL and pCL were constructed by inserting luc cDNA downstream of the HSV-*tk* and CAG (comprised of cytomegalovirus enhancer and chicken β-actin promoter) promoters, respectively. For expression of EGFP, we constructed pTE plasmid by inserting EGFP cDNA downstream of the HSV-*tk* promoter. pCE-29 plasmid (Sato et al., 2002), a CAG promoter-driven EGFP expression plasmid, was also used as a positive vector for expression of EGFP in murine cells. All junctions were confirmed by sequencing.

Cells and Transfection

NIH3T3 cells were first seeded onto 6-well gelatin-coated dishes (#4810-020; Iwaki Glass Co., Tokyo, Japan) at a density of 10^6 cells/well 1 day before transfection and grown in Dulbecco's modified Eagle's medium (DMEM; Invitrogen Co., Carlsbad, CA) supplemented with 10% fetal bovine serum (FBS; Invitrogen Co.) at 37°C in an atmosphere of 5% CO_2 in air at 37°C. For transfection of a single plasmid, four μg of plasmid DNA was mixed with 8 μl of Lipofectamine 2000 (#11668-027; Invitrogen Co.) in Dulbecco's modified phosphate-buffered saline without Ca^{2+} and Mg^{2+}, pH 7.4 [PBS(−)], and a total of 100 μl solution was prepared according to the manufacturer's protocol. For co-transfection, two plasmids (3 μg for each) + phRL-SV (0.03 μg; Promega Co., Madison, WI) were mixed with 12 μl of Lipofectamine 2000 in PBS(−). For transfection using a single vector, six μg of vector + phRL-SV (0.03 μg) were mixed with 12 μl of Lipofectamine

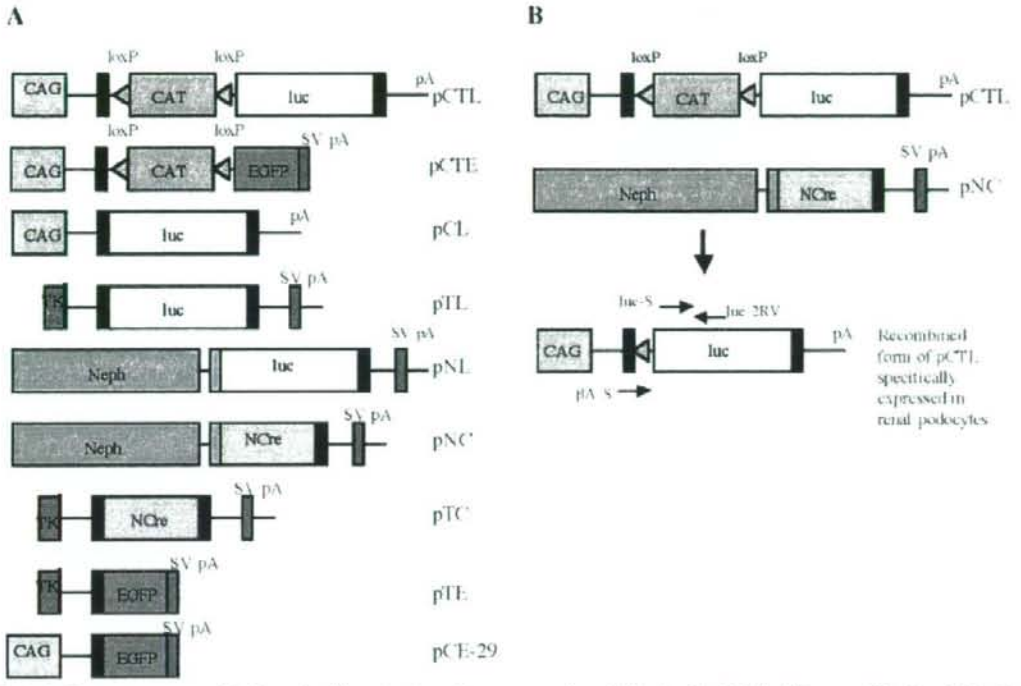

Fig. 1. A: Gene constructs used in this study. All constructs contain the 2nd intron, 3rd exon, and 3'-noncoding region from rabbit β-globin (indicated by black solid line) or 1st intron of chicken β-actin gene (indicated by blue solid line). Luciferase and EGFP cDNAs were used as reporter genes. To stop mRNA synthesis, all constructs contain poly(A) sites from rabbit β-globin or SV40 gene. CAG, cytomegalovirus enhancer + chicken β-actin promoter; CAT, chloramphenicol acetyltransferase gene; EGFP, enhanced green fluorescent protein cDNA; luc, luciferase cDNA; NCre, nuclear location signal + Cre gene; Neph, nephrin promoter + noncoding 1st exon + 1st intron + a portion of 2nd exon; pA, poly(A) site of rabbit β-globin gene; SV pA, poly(A) sites of SV40 gene; TK, HSV-*tk* promoter. **B**: Schematic representation of Cre-mediated recombination in pCTL. Before recombination, the *loxP*-flanked CAT sequence is expressed under control of the CAG promoter in cells carrying pCTL, while the luc cDNA is silent. When co-transfection of pCTL and pNC is performed for renal tissues, Cre-mediated recombination will result in deletion of the CAT sequence and expression of luc cDNA in a podocyte-specific manner. Arrows above and beneath the construct indicate primers used for PCR.

2000 and used. These DNA/liposome complexes were added to the cell culture and incubated for 1 day at 37°C. After transfection, cells were observed for fluorescence, as described below. Transfections were performed in triplicate.

Observation for Fluorescence

Cells were observed using an Olympus BX60 fluorescence microscope (Olympus, Tokyo, Japan) with DM505 filters (BP460-490 and BA510IF), which were used for EGFP monitoring. For detection of fluorescence in dissected oviducts, an Olympus BX40 dissecting microscope was used. Microphotographs were taken using a digital camera (FUJIX HC-300/OL; Fuji Film, Tokyo, Japan) attached to the fluorescence microscope and printed out using a Mitsubishi digital color printer (CP700DSA; Mitsubishi, Tokyo, Japan). Images captured using the digital camera were imported into Adobe photoshop for assembly of the final figures.

FACS Analysis

Twenty-four hours after transfection, the cells were washed twice with PBS(−) and dissociated with trypsin/EDTA. After centrifugation, the cells were resuspended at 3×10^6 cells/ml in PBS(−)/0.1% FBS and stored on ice for a maximum of 1 hr before analysis. Then 2 μg/ml of propidium iodide (PI; Sigma Co. Ltd.) was added immediately prior to flow cytometry. Acquisition was performed on a FACSCalibur system (BD Bioscience, Heidelburg, Germany) and samples were analyzed using Cell Quest Pro software (BD Bioscience). In each experiment, 10,000 counts were evaluated. Cells exhibiting PI uptake were considered dead and excluded from analysis of EGFP-positive cells by gating on PI-negative cells.

PCR Analysis

Isolation of genomic DNA from transfected oviducts was performed as previously described (Sato et al.,